Contents

This document contains the following items of Electronic Supplementary Material:

1. Supplementary Table S1;
2. Supplementary Figures S1 and S2;
3. Validation of the use of antennal tracking to estimate head roll, including Figures S3 and S4;
4. Sensitivity analysis for model of motion vision system, including Figures S6 and S6.

Table S1. Parameters of model Reichardt array

variable	value
interommatidial angle ($\Delta\psi$)	1.0°
acceptance angle†	2.0°
spatial high-pass filter constant†	0.0075
temporal low-pass filter time constant†	46ms
delay time constant (τ)†	46ms

†free parameter fitted to electrophysiological data [1].

References

1. Theobald JC, Warrant EJ & O'Carroll DC. 2010 Wide-field motion tuning in nocturnal hawkmoths. *Proc. Roy. Soc. B* **277**, 853–860.

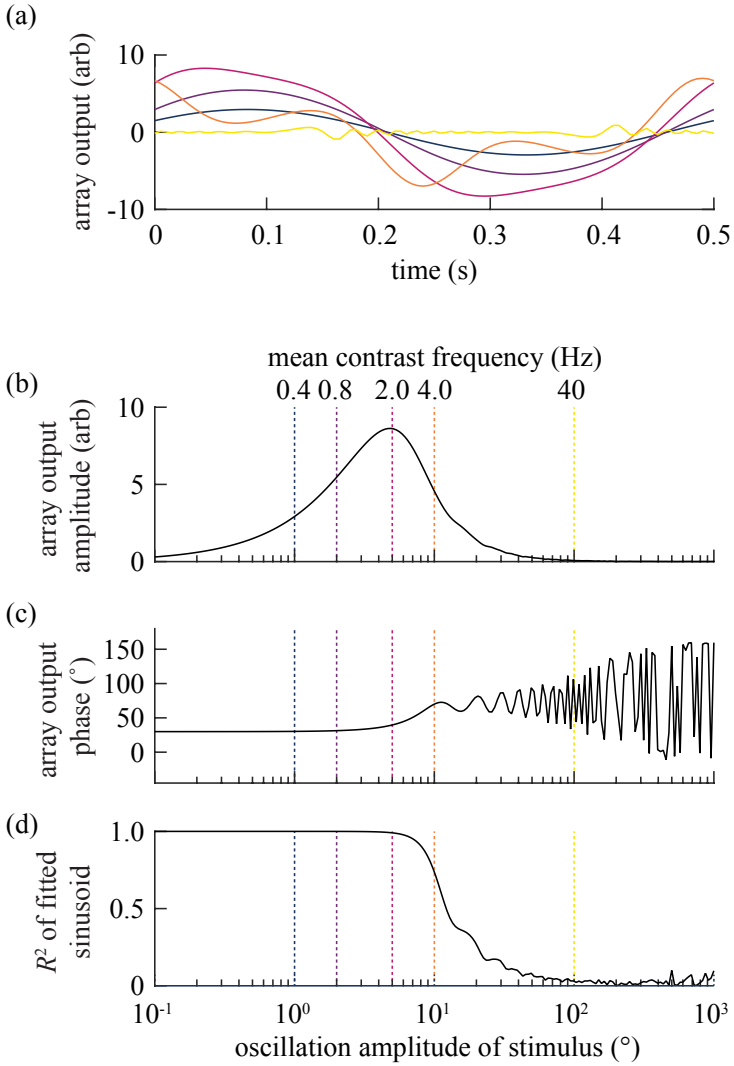


Figure S1. Distortion of the time-varying output of the model Reichardt array at high contrast frequencies. The plots show how the summed output of the model Reichardt array varies in response to a sinusoidal grating oscillating sinusoidally at each of five different oscillation amplitudes $A \in \{1°, 2°, 5°, 10°, 100°\}$. The oscillation frequency and spatial frequency of the stimulus were set at reference values of $f = 2$Hz and $S = (20°)^{-1}$, and the head was assumed to be held fixed. (a) Time-varying output of the Reichardt array (arbitrary units), for the five different stimulus amplitudes (coloured lines). The meaning of the colour coding is indicated by the dashed vertical lines on the plots beneath, from which can be read the oscillation amplitude and mean contrast frequency of the stimulus. Note that the sinusoidal oscillations of the visual stimulus only elicit a sinusoidal output at the lowest oscillation amplitudes, which are associated with the smallest range of contrast frequency and the lowest mean contrast frequency. (b,c) The amplitude and phase of the summed output were determined by fitting a simple sinusoid at the stimulus frequency to the time-varying output of the array. Note the pronounced phase shift and eventual instability at high contrast frequencies. (d) The R^2 value measures the goodness of fit of the sinusoid, which quickly declines as the output becomes distorted at high contrast frequencies.

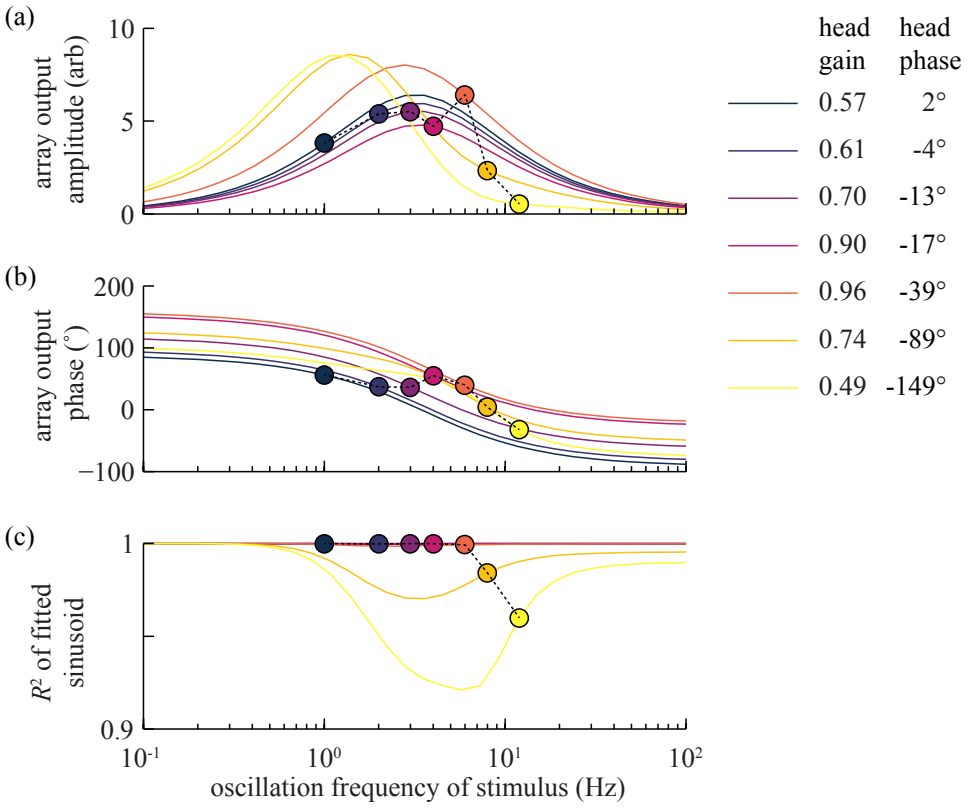


Figure S2. Effects of phase shift on the output of the model Reichardt array, illustrated for the responses measured in the tests varying the oscillation frequency of the visual stimulus. The coloured lines show the output (arbitrary units) that would result if the gain and phase of the compensatory head movement measured in response to a given stimulus were maintained across all stimulus frequencies. The similarly coloured circles denote the output predicted for the stimulus frequency at which the corresponding head movement response was actually measured. (a,b) The amplitude and phase of the summed output were determined by fitting a simple sinusoid at the stimulus frequency to the time-varying output of the array. (c) The R^2 value measures the goodness of fit of the fitted sinusoid. Note that whilst the effect of the compensatory head movements was to reduce the retinal slip speed at all but the 8 and 12Hz stimulus frequencies, the consequent attenuation of the effective contrast frequency was only sufficient to bring it below the peak in the Reichardt array's response at stimulus frequencies $\leq$ 3Hz. This is indicated by the coloured circle falling to the left of the peak in the same-coloured line. At stimulus frequencies $\geq$ 4Hz, the Reichardt array was still being pushed beyond the peak in its response curve, which is indicated by the coloured circle falling to the right of the peak in the same-coloured line. This pattern reflects the phase shift occurring with increasing oscillation frequency, and is the cause of the irregular form of the modified response curve shown by the black dashed line connecting the coloured circles.

Validation of the use of antennal tracking to estimate head roll

A potential limitation of this study is that we did not directly measure the motion of the insects' eyes relative to the motion of the visual stimulus: instead, we used the angle of the line joining the tips of the antennae in the video images as a proxy for the roll angle of the head, and hence the eyes. The antennal flagellum can be rotated about its base by muscles located in the head, scape, and pedicel [ref. 7 of main text], however, so if the antennae were to move independently of the head, then clearly this could degrade or alter the resulting estimates of the head's response magnitude and phase. Here we evaluate and validate our method of using the tilt of the line between the tips of the antennae as an estimate of the roll angle of the head.

To test whether the antennae moved independently of the head in response to the stimuli that we presented, we examined the effect of tracking different points on the antennae, instead of tracking only their tips. Clearly, if the antennae were to remain fixed with respect to the head, then the head and antennae would rotate together as a single rigid body, and by definition the measured angular velocity would be the same everywhere. Conversely, if the antennae were to move independently of the head, then they would no longer rotate together as a single rigid body, and the measured angular velocity would be different for different tracked points on the antennae. Because antennal movements occur as rotations about the base of the flagellum, it follows that the resulting discrepancy between the true angular motion of the head and the estimate obtained from the antennae should be greatest for tracked points closest to the tips of the antennae, and least for tracked points closest to the base (see Fig. S3 in this Appendix).

For antennal motions unrelated to the visual stimulus, the effect of such movements will be simply to add noise to the measurements, and hence to reduce the coherence of the estimated head response. Conversely, for antennal motions made in response to the visual stimulus, the effect will be to modify the magnitude and/or phase of the estimated head response. This being so, we would expect any coherent movements of the antennae to produce a systematic change in our estimate of the head's response magnitude or phase, according to the distance of the tracked point from the antenna tip. On the other hand, if the antennae were either to remain fixed with respect to the head, or to move in a manner unrelated to the visual stimulus, then we should expect to see no systematic variation in our estimate of the head's response magnitude and phase according to the distance of the tracked point from the antenna tip.

The centreline of each antenna was found by thresholding each video frame to give a binary image, skeletonizing the image, and then finding the shortest branch between the antenna tip and the junction with the outline of the head. This centreline was then used to define a series of points offset by differing distances from the antenna tip, and the motion of these offset points was calculated in the same way as for the antenna tips. Although there was naturally some variability in the resulting estimates of head roll angle, we found that the gain, phase, and coherence of the response did not vary much according to the distance of the tracked points from the tips of the antennae, and there was no evidence of any monotonic variation in our estimates of gain and phase with distance from the antenna tips (see Fig. S4 in this Appendix) It follows that any movements that the antennae may have made with respect to the head were not made in response to the visual stimulus, and hence that the rotation of the line joining the antenna tips may indeed be used to determine the response properties of the head. This validates our method of estimating the change in the roll angle of the head from the change in the angle of the line joining the tips of the antennae in the video of the moth.

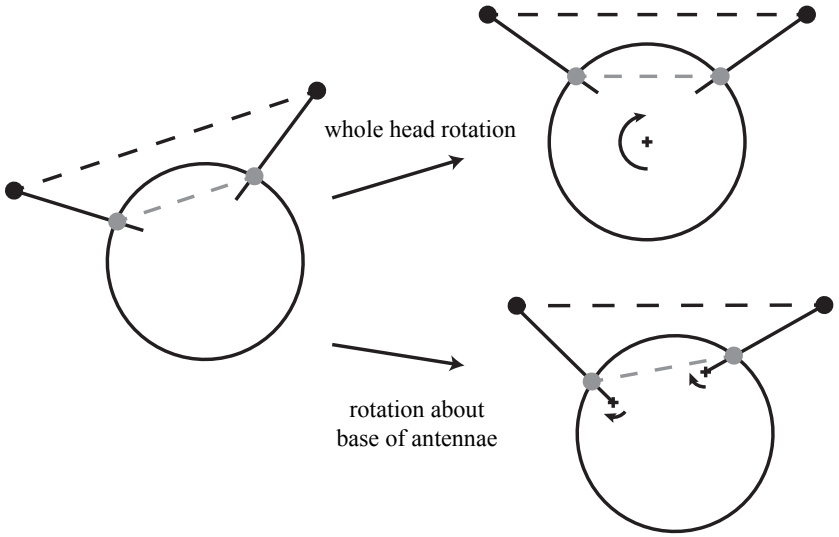


Figure S3. Schematic showing how the rotation of the line joining the tracked points on the antennae is affected by possible movements of the antennae with respect to the head, for two different positions of the tracked points. If the antennae are fixed with respect to the head, then the change in the angle of the line joining the tracked points is expected to remain constant as the position of the tracked points is moved from the tip (black circles) to base (grey circles) of the antennae. If instead the antennae rotate with respect to the head, then the measured change in the angle of the line joining the tracked points is expected to vary systematically as the position of the tracked points is moved from the tip (black circles) to base (grey circles) of the antennae. It follows that we can test whether or not the antennae rotate with respect to the head in response to the visual stimulus by comparing the magnitude and phase of the head response that we estimate when tracking different points on the antennae. See text for further explanation.

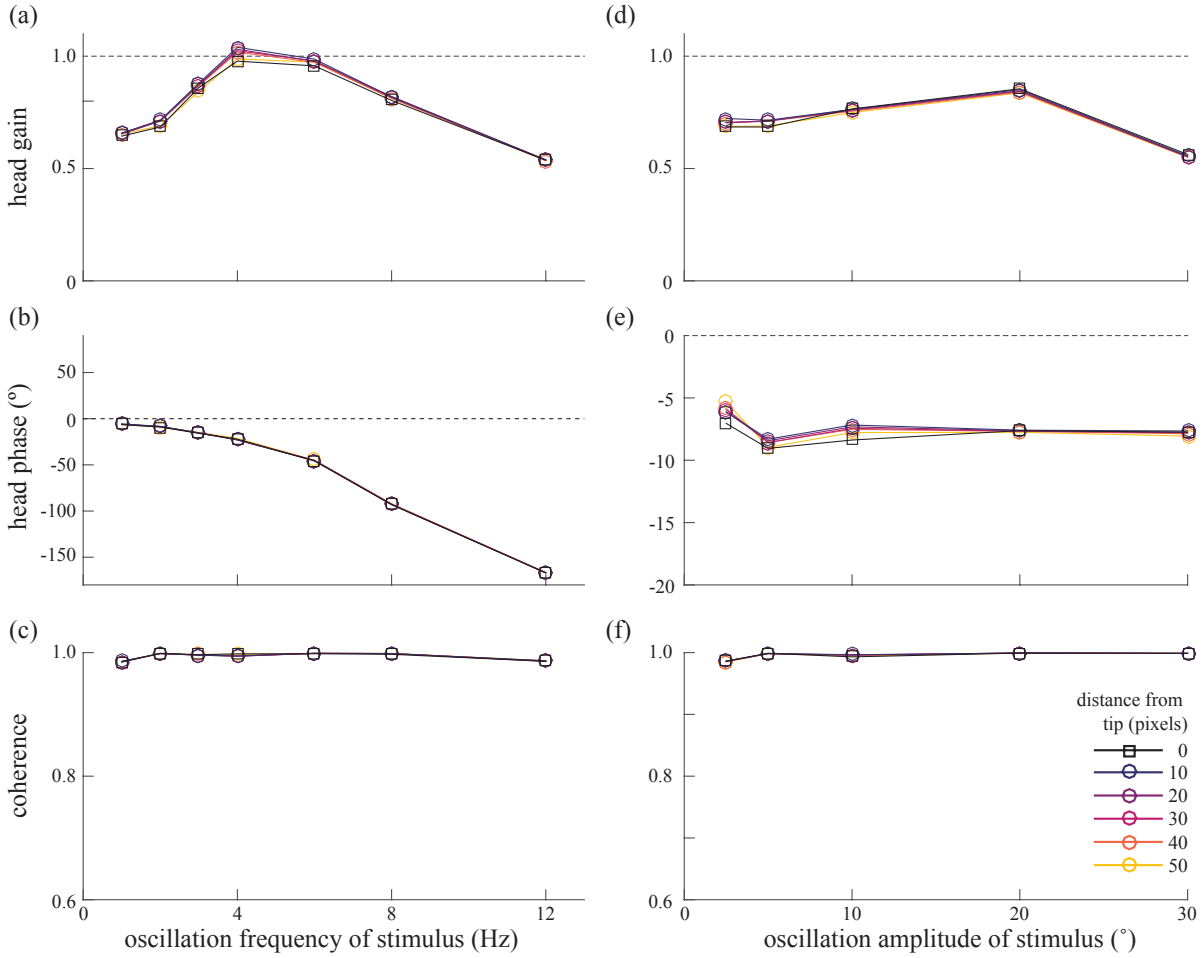


Figure S4. Head movement response for an individual moth estimated from the motion of different control points on the antennae, in response to the tests varying the oscillation frequency (a-c), and oscillation amplitude (d-f) of the visual stimulus. The colours of the lines indicate the distance of each control point from the antenna tip. As in the main text, the gain, phase, and coherence of the response refer to the roll angle of the head relative to the angular position of the stimulus. Note that although the measurements naturally show some variability, the discrepancies are small, and there is no evidence of any monotonic variation in our estimates with distance from the antenna tips. We therefore conclude that the antennae were not moving independently of the head in response to the stimulus, in which case the signal to noise ratio is expected to be best at the antenna tips, where the effect of any digitization error will be smallest.

Sensitivity analysis of model of moth motion vision system

To check the sensitivity of our results to the input parameters of the EMD model, we tested a series of alternatively tuned models. One model had input parameters which simulated a slower, lower resolution optical system, with twice the acceptance angle, twice the temporal low pass filter time constant, twice the delay time constant, and half the spatial high-pass filter constant, as compared to the tuned baseline model. The other model had input parameters which simulated a faster, higher resolution optical system, with half the acceptance angle, half the temporal low pass filter time constant, half the delay time constant, and twice the spatial high-pass filter constant. The effect of these changes on the summed response of the EMD array is shown in Fig. S5. Both alternatively tuned models were then tested in the same way as the tuned baseline model, inputing the experimentally measured head motions to look at the effect of head motions on the output of the EMD array. The two alternatively tuned models both had lower amplitude outputs than the tuned baseline model in response to the stimuli that we presented (Fig. S6), which is to be expected in light of their different tuning curves (Fig. S5), given that we used stimuli designed to elicit a maximal response from the EMD array of *Hyles lineata*, to which the baseline model was tuned. Nevertheless, both alternatively tuned models produced qualitatively the same result as the tuned model (Fig. S6), in that the measured compensatory head motions always increased the effective working range of the motion vision system in relation to the velocity of the visual stimulus. Indeed, the enhancement of the effective working range of the motion vision system was in fact even greater for the slower, lower resolution EMD array. This confirms that the qualitative conclusions that we draw from the tuned model are robust to model uncertainty in the tuning of the EMD input parameters, and can naturally be generalised from the specific case that we study here.

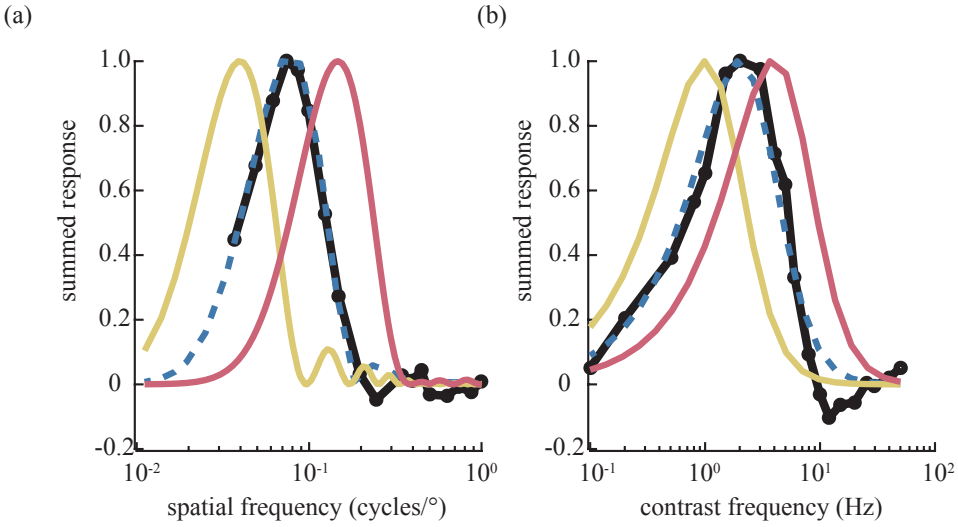


Figure S5. Open-loop response curves of three alternatively tuned models of the EMD array. The response curves for the slower EMD array (tan line), the faster EMD array (red line), and the tuned baseline model (dashed blue line), are shown in comparison with the electrophysiological data for *Manduca sexta* to which the baseline model was tuned (black line). Response plotted as a function of: (a) spatial frequency; (b) contrast frequency.

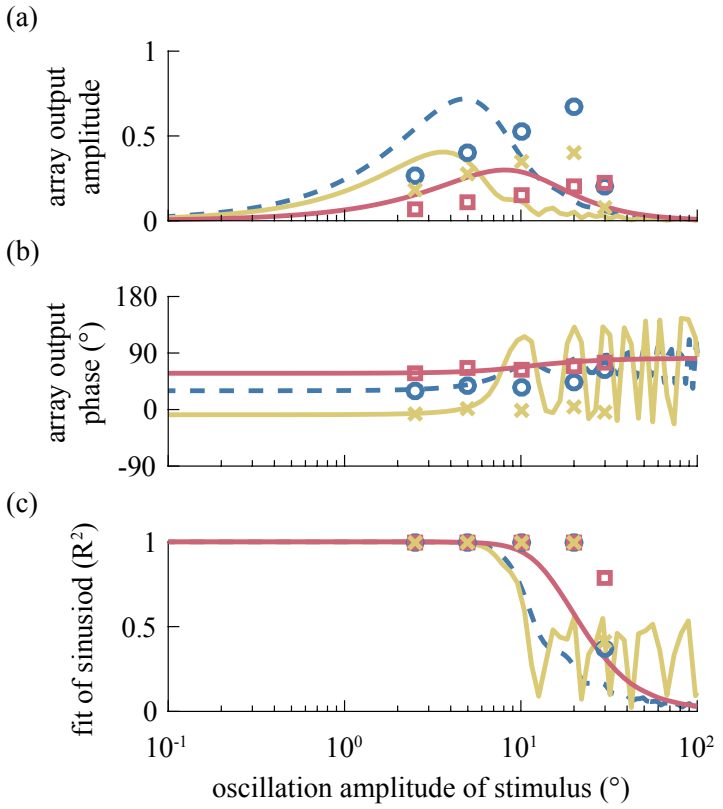


Figure S6. Open-loop versus closed-loop response of three alternatively tuned models of the EMD array in tests varying the amplitude of the visual stimulus for the slower EMD array (tan line and crosses), the faster EMD array (red line and squares), and the tuned baseline model (dashed blue line and circles). Plotted lines show the response with the head held fixed; point markers show the response assuming the same gain and phase of head motion as was measured experimentally under each test condition. The amplitude, phase, and R^2 were determined by fitting a sinusoid at the stimulus frequency to the output of the array. The amplitude of the responses are in arbitrary units, with all models being scaled by a common factor for comparability.